Journal of Catalysis 327 (2015) 58–64

Contents lists available at ScienceDirect

Journal of Catalysis

journal homepage: www.elsevier.com/locate/jcat

Unraveling the structure sensitivity in methanol conversion on CeO_2: A DFT + *U* study

Marçal Capdevila-Cortada [a,*], Max García-Melchor [a,b], Núria López [a,*]

[a] *Institute of Chemical Research of Catalonia (ICIQ), Av. Països Catalans, 16, 43007 Tarragona, Spain*
[b] *SUNCAT Center for Interface Science and Catalysis, SLAC National Accelerator Laboratory, Menlo Park, CA 94025, USA*

ARTICLE INFO

Article history:
Received 27 November 2014
Revised 16 March 2015
Accepted 19 April 2015

Keywords:
CeO_2
Structure sensitivity
Methanol oxidation
Formaldehyde oxidation
Dehydrogenation
H_2 formation
DFT
Reaction mechanisms

ABSTRACT

Methanol decomposes on oxides, in particular CeO_2, producing either formaldehyde or CO as main products. This reaction presents structure sensitivity to the point that the major product obtained depends on the facet exposed in the ceria nanostructures. Our density functional theory (DFT) calculations illustrate how the control of the surface facet and its inherent stoichiometry determine the sole formation of formaldehyde on the closed surfaces or the more degraded by-products on the open facets (CO and hydrogen). In addition, we found that the regular (100) termination is the only one that allows hydrogen evolution via a hydride–hydroxyl precursor. The fundamental insights presented for the differential catalytic reactivity of the different facets agree with the structure sensitivity found for ceria catalysts in several reactions and provide a better understanding on the need of shape control in selective processes.

1. Introduction

Cerium oxide, CeO_2, is a versatile and economically attractive oxide used in solid oxide fuel cells [1], biomedicine [2], and catalysis [3]. Either as a catalyst or as a support, it is widely used in a vast number of oxygen-related reactions such as the water–gas shift (WGS) [4,5], the preferential oxidation of CO [6,7], SO_2 oxidation [8,9], and the HCl conversion to Cl_2 [10]. All these applications are due to the particular redox character of ceria that permits to cycle between the Ce^{4+} and Ce^{3+} states, which involves oxygen vacancy formation [11] and diffusion [10,12]. The oxygen storage capacity (OSC) of CeO_2 varies with the exposing surface [13], and hence, in nanoparticles it ultimately depends on their morphology.

Recently, ceria has been also shown to present a high activity and selectivity in hydrogenation processes [10,14]. More surprisingly, the oxidation and hydrogenation capacities of different nanostructured CeO_2 materials have been found to present a markedly structure sensitivity [15]. Thus, while hydrogenation takes place preferentially on (111) facet orientations, oxidation reactions are favored on the more open (110) and (100) facets exposed in rods and cubes, respectively. Ceria nanoparticles have also been found to exhibit different activities in soot combustion depending on the exposed facet [16].

Among oxidation processes, the conversion of methanol to formaldehyde is considered an ideal test for characterizing the catalytic behavior of metal oxides [17,18]. The two main by-products of this reaction are water and hydrogen. Therefore, the catalytic activity and selectivity of a given material may be a result of the interplay between its oxidation and hydrogenation abilities.

In industry, methanol is oxidized to produce formaldehyde through the so-called Formox process [19]. There, methanol and oxygen react at temperatures around 525–675 K in the presence of iron oxide mixed with molybdenum or vanadium oxide according to the following equations:

$$CH_3OH + 1/2O_2 \rightarrow HCHO + H_2O \quad (1)$$

$$CH_3OH \rightarrow HCHO + H_2 \quad (2)$$

At higher temperatures, 875 K, silver can also act as catalyst, probably in the form of a suboxide [20–22]. Hence, the oxidation of methanol to formaldehyde has been extensively studied on metal oxides, especially on titanium and vanadium oxides [23–28]. In the case of ceria, most of the investigations have been focused on the (111) facet [29–33]. On this stoichiometric surface, methanol converts into formaldehyde, at *ca.* 550 K, via a dehydrogenation process that involves surface oxygens followed by the

---

* Corresponding authors.

E-mail addresses: mcapdevila@iciq.es (M. Capdevila-Cortada), nlopez@iciq.es (N. López).

http://dx.doi.org/10.1016/j.jcat.2015.04.016
0021-9517/© 2015 Elsevier Inc. All rights reserved.

subsequent reduction of two Ce^{4+} ions per methanol molecule [29]. The presence of oxygen vacancies was recently reported to have a detrimental effect on the reaction selectivity as a result of the competition between formaldehyde desorption and its further oxidation to CO [34]. In the same work, the (100) surface was also shown to have a reduced selectivity toward formaldehyde. Both HCHO and CO were found to be the main products on $CeO_2(100)$, while on the reduced $CeO_x(100)$ almost all methanol was converted to CO [34]. Temperature-programmed desorption (TPD) experiments on nanocrystals with different nanoshapes, namely octahedra, cubes, and rods, showed that the latter is the most reactive shape (but non-selective to formaldehyde) one, evolving CO and H_2 at $T < 583$ K [35]. On the other hand, Zhou and Mullins reported that formaldehyde does not decompose on stoichiometric $CeO_2(111)$, but does evolve to CO and H_2 on the same reduced surface at temperatures above 500 K [36]. Overall, ceria appears to be very sensitive to the particular choice of active surfaces.

Despite all the above and other theoretical works reported in the literature [37–42], up to date there is no complete study assessing the selectivity of methanol dehydrogenation on the most representative ceria facets and proving their different behavior as experimentally observed. Herein, we present a thorough mechanistic study on the selective conversion of methanol to formaldehyde and its subsequent conversion to CO. To account for the particular morphology of the three common nanoshapes above, we have studied the three lowest index and energy surfaces (111), (110), and (100) (Fig. 1), as these are the most exposed facets in each nanoshape, respectively. The desorption of HCHO, CO, and H_2 from each surface is also discussed and compared to the reported TPD results on the stoichiometric ceria surfaces [29,33,34]. Overall, this work provides the clues behind the structure sensitivity in the aforementioned oxidation process.

2. Computational details

All the calculations reported in the present study were performed at the DFT + U level using the Vienna *Ab initio* Simulation Package (VASP, version 5.3.3) [43,44]. The Perdew–Becke–Ernzerhof (PBE) [45] functional was used in combination with an effective U term, U_{eff}, of 4.5 eV (this term is defined as the difference between the Coulomb, U, and the exchange, J, terms) [46], as it has been previously proven to provide satisfactory results [47–50]. The purpose of adding this Hubbard term U is to diminish the self-interaction error and to properly localize the Ce 4*f* states. Projector-augmented wave (PAW) pseudopotentials [51] were used to describe the core electrons with a plane-wave cutoff energy of 500 eV for the valence electrons (*i.e.*, 5*s*, 5*p*, 4*f*, 6*s* for Ce atoms, and 2*s*, 2*p*, for O and C atoms).

Ceria presents a fluorite structure, with lattice parameter $a_{exp} = 5.411$ Å [52]. We optimized the lattice parameter using a dense Γ-centered $7 \times 7 \times 7$ k-point mesh, leading to the value $a_{calc} = 5.497$ Å, in good agreement with both the experimental value and previous computational studies [53]. To maintain the stoichiometry of the $CeO_2(100)$ surface and avoid the dipole moment normal to the surface, a half oxygen monolayer was transferred from the surface to the bottom of the slab [54]. The (111), (110), and (100) surfaces were modeled as (2×2) periodically repeated slabs consisting of four, five, and three O–Ce–O layers, respectively, separated by 15 Å of vacuum space, and were optimized using a Γ-centered k-point mesh denser than 0.38 $Å^{-1}$. The layers allowed to relax in each surface were the five outermost layers in $CeO_2(111)$, the three top-most layers in $CeO_2(110)$, and the four outermost layers in $CeO_2(100)$, whereas the rest of atoms were kept fixed to their bulk positions.

Transition states were located by means of the climbing image nudged elastic band (CI-NEB) method [55]. The nature of all reaction minima and transition states was confirmed by means of numerical frequency analyses.

3. Results

3.1. Dehydrogenation of methanol to formaldehyde on CeO_2

We investigated the conversion of methanol to formaldehyde on the three lowest energy surfaces corresponding to the low-index planes (111), (110), and (100). Their surface and relaxation energies are presented in the Supplementary Material (Table S1).

The reaction consists in the sequence of the following elementary steps:

$$CH_3OH + {}^* \rightarrow CH_3OH^* \tag{R1}$$

$$CH_3OH^* + {}^* \rightarrow CH_3O^* + H^* \tag{R2}$$

$$CH_3O^* + {}^* \rightarrow HCHO^* + H^* \tag{R3}$$

$$HCHO^* \rightarrow HCHO + {}^* \tag{R4}$$

Methanol physisorbs on ceria (R1) and dissociates (R2) giving rise to a chemisorbed methoxy and surface OH groups. The methoxy intermediate then leads to formaldehyde through a C–H bond breaking (R3) with the concomitant hydrogenation of another surface oxygen. Finally, formaldehyde desorbs from the surface to the gas phase (R4).

Reaction (R2) is controlled by the acid–base properties of the surface and does not involve any change in the oxidation state of the reactant fragments or the surface metal atoms. In contrast, reaction (R3) can be seen as the main redox step as two Ce^{4+} cations are reduced to Ce^{3+} after the C–H scission and the subsequent formation of a second surface OH group. The discrimination in terms of acid–base and redox steps has been recently found to be crucial to tune the catalytic activity of oxides [56].

The calculated energy profiles for the methanol to formaldehyde conversion on the different CeO_2 surfaces are presented in

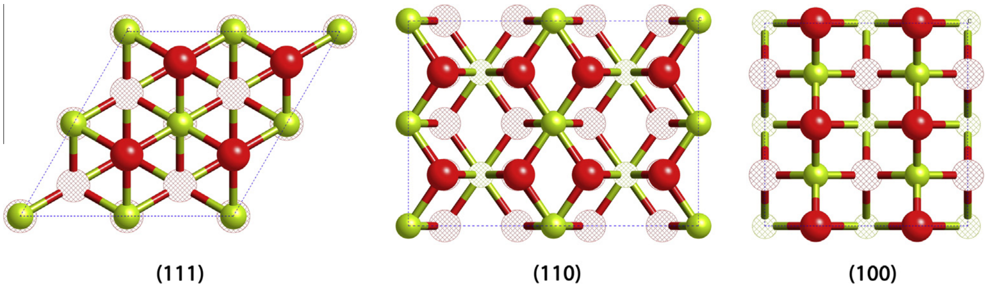

Fig. 1. Top views of the three lowest index CeO_2 surfaces. The outmost oxygen (in red) and cerium (in green) layers are highlighted, while the rest of atoms are shown dashed. (For interpretation of the references to color in this figure legend, the reader is referred to the web version of this article.)